Physics of the Solid State, 2024, Vol. 66, No. 4

03,08

Magnetoresistance oscillations in films of multicomponent topological insulators based on bismuth telluride

© L.N. Lukyanova, O.A. Usov, M.P. Volkov

Ioffe Institute,
St. Petersburg, Russia

E-mail: lidia.lukyanova@mail.ioffe.ru

Received March 8, 2024
Revised March 8, 2024
Accepted March 14, 2024

In layered films of n-$(Bi, Sb, In)_2(Te, Se)_3$ solid solutions, which are 3D topological insulators, quantum oscillations and temperature dependences of magnetoresistivity have been investigated in strong magnetic fields up to 14 T. Using the Lifshitz−Kosevich theory, the parameters of the surface states of Dirac fermions have been calculated, revealing that the studied films are characterized by two cyclotron resonance frequencies. It is demonstrated that the surface concentration of Dirac fermions increases in films with a high thermoelectric power factor when substituting atoms in the Bi sublattice with In, compared to Sb → Bi substitutions. The Landau level indices and Berry phase have been calculated. It is demonstrated that with an increase in the cyclotron resonance frequency in the film n-$Bi_{1.92}In_{0.02}Te_{2.88}Se_{0.12}$, Landau levels are observed at higher magnetic fields compared to n-$Bi_{1.6}Sb_{0.4}Te_{2.91}Se_{0.09}$. In the n-$Bi_{1.6}Sb_{0.4}Te_{2.91}Se_{0.09}$ films, temperature dependencies of resistivity in the magnetic field $B = 14$ T exhibit plateaus at low temperatures, characteristic of topological insulators. At temperatures below 15 K, a non-linear dependence of resistivity on magnetic field is observed due to quantum interference effects associated with weak anti-localization of Dirac fermions.

Keywords: thermoelectrics, layered films, quantum oscillations, strong magnetic fields, surface states.

DOI: 10.61011/PSS.2024.04.58197.47

1. Introduction

Layered films of solid solutions of n-$(Bi, Sb, In)_2/(Te, Se, S)_3$ are effective thermoelectrics with a tetradimite structure and belong to strong topological 3D-insulators (TI) with surface 2D states of Dirac fermions [1–3]. Topological surface states in these materials arise as a result of the inversion of electronic states at the edges of the band gap and are associated with strong spin-orbit interaction. Anomalous spin-dependent metallic conductivity and spiral-spin texture are characteristic of Dirac fermions [1,2].

Currently, intensive studies of chalcogenide thermoelectrics are carried out to use topological surface states in electronic technologies, in photonics, and in optical communication systems [4–6]. The absence of backscattering on non-magnetic impurities in TI contributes to an increase of the mobility, which stimulates the creation of energy-efficient field-effect transistors based on films of $Bi_2Se_3$and Bi_2Te_3 [4,7,8]. The use of Bi_2Te_3 films for information processing using magnetic devices that can be competitive in speed and performance with available modern technologies is promising [4]. Films of Sb_2Te_3, GeTe, $Ge_2Sb_2Te_5$ compounds are used for the development of neuromorphic materials and devices [9].

In thermoelectricity, the use of the properties of surface states of fermions is associated with the effect of superfluidity of surface topological excitons in Sb_2Te_3/Bi_2Te_3 heterostructures containing p−n-transition [10,11].

The impact of Dirac fermions on an increase of the power factor in p-$Bi_{05}Sb_{1.5}Te_3$ films of submicron thickness was observed in isostructural topological transitions [12,13] at high pressures, $P = 3{-}4$ GPa. A significant increase of the power factor under pressure compared to normal conditions determines the prospects for the use of films of p-$Bi_{05}Sb_{1.5}Te_3$ as a p-branch of thermoelectric devices [12]. The characteristics of the developed devices can be improved in a magnetic field owing to the additional transverse and longitudinal magneto-thermoelectric effects [14].

The galvanomagnetic effects measured in strong magnetic fields [15–17] constitute an informative method for analyzing the topology of thermoelectrics of bismuth and antimony chalcogenides. This paper studies the quantum oscillations effects of magnetoresistance in magnetic fields up to 14 T at low temperatures and the dependence of magnetoresistance on temperature up to room temperature in films of solid solutions of n-$Bi_{1.6}Sb_{0.4}Te_{2.91}Se_{0.09}$.

2. Quantum oscillations of magnetoresistance

Periodic quantum oscillations of magnetoresistance amplitudes in strong magnetic fields at low temperatures, resulting from modulation of the density of electron states with a cyclotron resonance frequency F, are used to calculate the parameters of the surface states of Dirac fermions in TI [18–20].

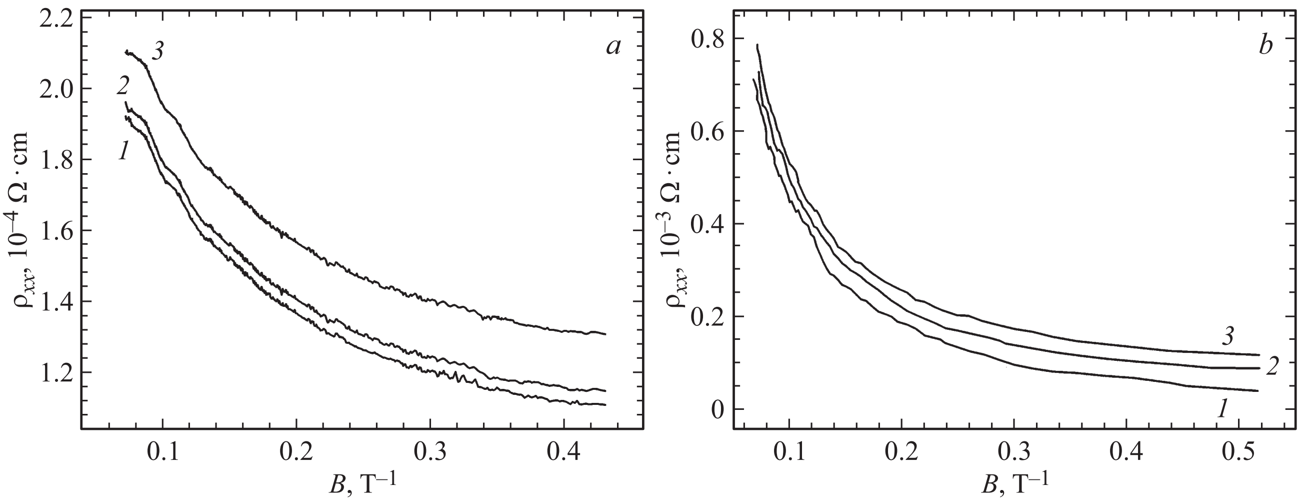

Figure 1. Resistivity ρ_{xx} (curves *1–3*) depending on the reverse magnetic field B^{-1} in films of *a*) n-$Bi_{1.92}In_{0.02}Te_{2.88}Se_{0.12}$ and *b*) n-$Bi_{1.6}Sb_{0.4}Te_{2.91}Se_{0.09}$ at temperatures of T, K: *1* — 3, *2* — 5, *3* — 10.

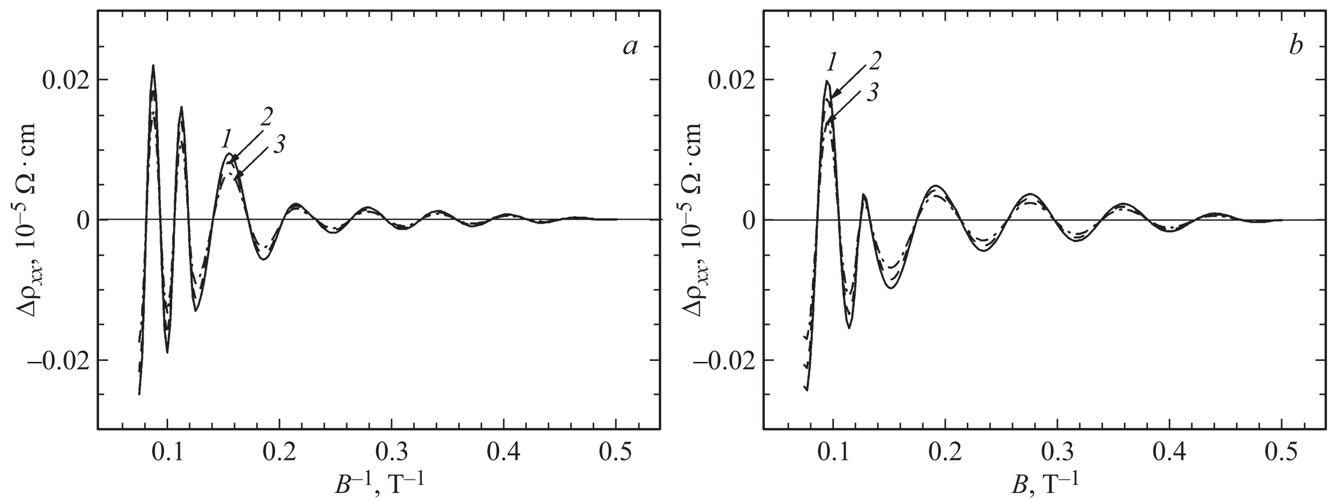

Figure 2. Quantum oscillations of magnetoresistance $\Delta\rho_{xx}$ (curves *1–3*) depending on the reverse magnetic field B^{-1} in films of *a*) n-$Bi_{1.92}In_{0.02}Te_{2.88}Se_{0.12}$ and *b*) n-$Bi_{1.6}Sb_{0.4}Te_{2.91}Se_{0.09}$ for temperatures T, K: *1* — 3, *2* —5, *3* — 10.

The layered films of solid solutions of n-$Bi_{1.92}In_{0.02}Te_{2.88}Se_{0.12}$ and n-$Bi_{1.6}Sb_{0.4}Te_{2.91}Se_{0.09}$ were prepared for the study by exfoliation of single crystal grains of bulk materials up to 500 nm using the method described in [21]. The dependences of the resistivity ρ_{xx} on the magnetic field were measured on the obtained films, on a substrate made of sticky polymer tape (Figure 1) using the unit of the Physical Property Measurement System (PPMS) Transport Option in the low temperature range of $T < 10$ K in magnetic fields of up to 14 T. The current I was directed along, and the magnetic field B — was perpendicular to the interlayer surface of van der Waals (0001) during the measurements, which corresponds to transverse magnetoresistance.

The frequencies of cyclotron resonance F_1 and F_2 in layered films (Figure 3) were determined from the dependences of oscillations $\Delta\rho_{xx}(B^{-1})$ (Figure 2) using the fast Fourier transform method. Figure 3 shows that the spectral values of amplitude A of quantum oscillations of magnetoresistance depending on the frequency of F in films have two resonant frequencies, F_1 and F_2. The appearance of two resonant frequencies in the studied films is determined by a change of the conditions of cyclotron resonance on the free surface of the film and the surface located on the substrate, as well as by the features of the Fermi surface [17]. As follows from Figure 3, the amplitudes of magnetoresistance oscillations A decrease with the increase of the temperature. Fermi level in films of similar composition n-$Bi_{1.6}Sb_{0.4}Te_{2.94}Se_{0.06}$ [22] and n-$Bi_{1.92}In_{0.02}Te_{2.85}Se_{0.15}$ [23] is located in the band gap, which confirms the contribution of surface carriers to quantum oscillations of magnetoresistance (Figures 2 and 3).

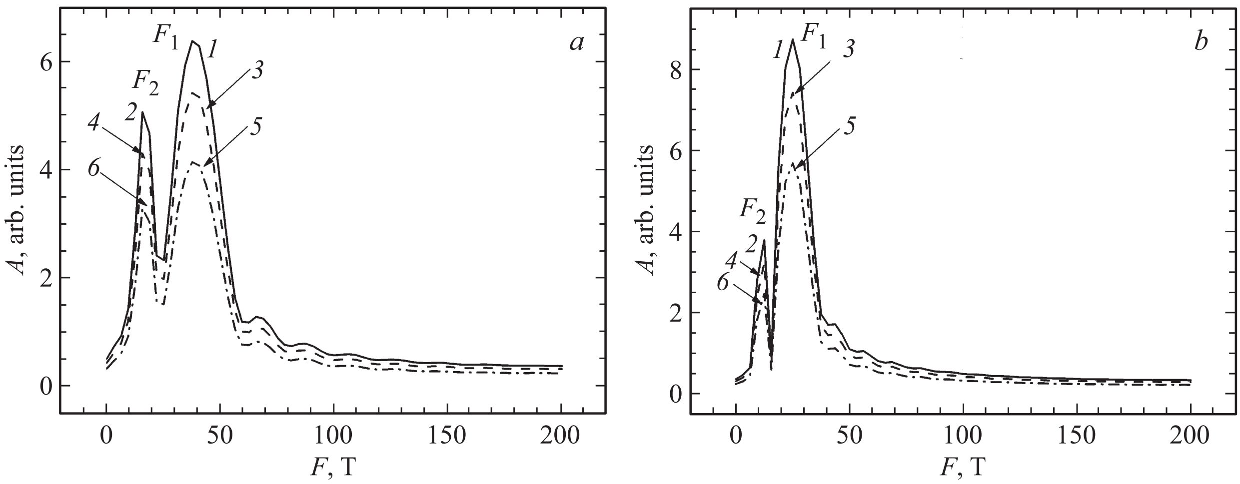

Figure 3. Amplitudes A of quantum oscillations of magnetoresistance depending on the frequency of cyclotron resonance F in film of a) n-$Bi_{1.92}In_{0.02}Te_{2.88}Se_{0.12}$ and b) n-$Bi_{1.6}Sb_{0.4}Te_{2.91}Se_{0.09}$. Curves *1, 2* — 3 K, *3, 4* — 5 K, *5, 6* — 10 K. The maximum frequencies of cyclotron resonance are: a — $F_1 = 38.5$ and $F_2 = 15.6$ T, b —$F_1 = 26$ and $F_2 = 12$ T.

3. Parameters of Dirac fermions

The cross-sectional area of the Fermi surface $S(k_F)$, the wave vector k_F and the surface concentration of fermions n_s for layered films were calculated from the magneto-resistance oscillation amplitudes $\Delta\rho_{xx}(B^{-1})$ (Figure 2, a and b) in accordance with Lifshitz–Kosevich theory [16,18,24,25]. Frequency of cyclotron resonance of oscillations

$$F = \left(\frac{\hbar}{2\pi e}\right) S(k_F), \quad (1)$$

$$k_F = \sqrt{\frac{S(k_F)}{\pi}}. \quad (2)$$

The surface concentration n_s is determined as follows: $n_s = k_F^2/(4\pi)$.

Since two resonant frequencies F_1 and F_2 were detected in the studied films (Figure 3), two sets of parameters correspond to them (Table).

The surface concentration of ns is one of the parameters that impacts the contribution of Dirac surface fermions to thermoelectric properties. The value of n_s in the film of n-$Bi_{1.92}In_{0.02}Te_{2.88}Se_{0.12}$ with high power factor $PF = 48 \cdot 10^{-6}\,W \cdot cm^{-1} \cdot K^{-2}$ at low temperatures was higher than in n-$Bi_{1.6S}Sb_{0.4}Te_{2.91}Se_{0.09}$with a smaller factor $PF = 29.3 \cdot 10^{-6}\,W \cdot cm^{-1} \cdot K^{-2}$ (table). It should be noted that the value of n_s in the film of n-$Bi_{1.92}In_{0.02}Te_{2.88}Se_{0.12}$ according to differential tunneling conductivity data, measured by scanning tunneling spectroscopy at room temperature is $2.8 \cdot 10^{12}\,cm^{-2}$ [23], which is significantly higher than n_s at low temperatures (table).

The Fermi level E_F (Table) corresponding to the higher frequency F_1 is located higher than at the lower frequency F_2 (Figure 3), therefore the frequency F_1 is associated with the upper free surface of the film, and F_2 is associated with the lower surface, which is located on the substrate, which is consistent with experimental studies of films based on bismuth telluride and antimony [17,26]. The higher frequency F_1 on the free surface of the studied films is confirmed by the results of comparison of data obtained by angular resolution photoelectron spectroscopy (ARPES) on the free surface of films at low temperatures and the study of oscillation effects in strong magnetic fields [17,26]. Measurements of the ARPES spectra showed that the values of the Fermi level E_F and the surface concentration n_s on the free surface of the films are consistent with similar data obtained from oscillation effects for a higher frequency of cyclotron resonance [17,26]. It follows from the data given in the table that E_F and n_s in films of n-$Bi_{1.92}In_{0.02}Te_{2.88}Se_{0.12}$ and n-$Bi_{1.6}Sb_{0.4}Te_{2.91}Se_{0.09}$ are higher on the free surface, as is the frequency of cyclotron resonance.

The cyclotron effective mass of fermions was calculated using the least-square method (LSM) m_{cyc} from the temperature dependences of $\Delta\rho_{xx}(B^{-1})$ (Figure 2), normalized by the amplitude of oscillations at $T = 3$ K, at a fixed maximum magnetic field $B = 14$ T. The velocity υ_F and Fermi energy E_F (table) were obtained from data of the effective mass m_{cyc} and the wave vector k_F in accordance with [16,25]. The fermion relaxation time τ and the Dingle temperature T_D were calculated at a minimum temperature $T = 3$ K from the slope angles of the maximum oscillation amplitudes $\Delta\rho_{xx}(B^{-1})$ and the reverse magnetic field (Figure 2). Free path length $l_F = \upsilon_F\tau$ and fermion mobility $\mu = e\tau/m_{cyc}$ [16,25]. The values of l_F and the mobility of fermions μ were determined using k_F, υ_F and m_{cyc}. The values l_F for two cyclotron frequencies F_1 and F_2 were higher in the film of n-$Bi_{1.92}In_{0.02}Te_{2.88}Se_{0.12}$, while the mobility of μ slightly increased compared to the film of n-$Bi_{1.6}Sb_{0.4}Te_{2.91}Se_{0.09}$ (table).

Parameters of the surface states of Dirac fermions

F, T	$S(k_F)$, nm^{-2}	k_F, nm^{-1}	E_F, meV	n_s, 10^{12} cm^{-2}	m_{cyc}/m_e	τ, 10^{-13} s	T_D, K	l_F, nm	υ_F, 10^5 m/s	μ, m^2/Vs
n-$Bi_{1.92}In_{0.02}In_{0.02}Se_{0.12}$										
38.5	0.368	0.342	81.0	0.93	0.11	3.06	3.98	110	3.6	0.489
15.6	0.149	0.218	24.1	0.38	0.15	2.44	4.96	41.0	1.68	0.286
n-$Bi_{1.6}Sb_{0.4}Te_{2.91}Se_{0.09}$										
26.0	0.248	0.281	46.3	0.63	0.13	4.5	2.7	84.0	2.50	0.454
12.0	0.115	0.191	16.3	0.29	0.17	4.5	2.7	35.0	1.30	0.278

4. Landau levels and Berry phase

The quantum oscillations of the magnetoresistance $\Delta\rho_{xx}(B^{-1})$ (Figure 2, *a* and *b*) are associated with the redistribution of the electron density of carriers at the Landau levels. The energy difference of the Landau levels corresponds to the cyclotron resonance frequency [18,19]. The extreme positions of oscillation amplitudes $\Delta\rho_{xx}$ on dependencies $\Delta\rho_{xx}(B^{-1})$ were used to construct a Landau diagram and determine the Berry phase (Figure 4) in films of n-$Bi_{1.92}In_{0.02}Te_{2.88}Se_{0.12}$ and n-$Bi_{1.6}Sb_{0.4}Te_{2.91}Se_{0.09}$ (Figure 2, *a* and *b*).

The Landau level indices n and the Berry phase β (Figure 4) were determined using LSM in accordance with the expression $n = F \cdot B_{\text{exs}}^{-1} + \beta$ [17.25] for cyclotron resonance frequencies F_1 and F_2 in the inverse magnetic fields B_{exs}^{-1}, which characterize the positions of the minima and maxima of the magneto-resistance oscillation amplitudes.

The Landau levels n were detected in the range of magnetic fields of $B = (13.7-8.8)$ T on the upper surface of the film of n-$Bi_{1.92}In_{0.02}Te_{2.88}Se_{0.12}$ for the cyclotron frequency of $F_1 = 38.5$ T. The whole indices of the Landau levels were equal to $n = 4$, 5, and the half-integer indices were equal to $n = 3.5$ and 4.5 (Figure 4, curve *1*). For the frequency $F_2 = 15.6$ T on the lower surface of the film of n-$Bi_{1.92}In_{0.02}Te_{2.88}Se_{0.12}$ integer indices $n = 5, 6$, and the half-integers — $n = 5.5$ and 6.5 at $B = (3.6-2.6)$ T (Figure 4, curve *2*).

The integer indices — $n = 3$, 4, 5 at $B = (10.2-5.75)$ T in the film of n-$Bi_{1.6}Sb_{0.4}Te_{2.91}Se_{0.09}$ on the upper surface for the frequency $F_1 = 26$ T, and half-integer indices — $n = 2.5$, 3.5, 4.5 at $B = (12.9-6.4)$ T (Figure 4, curve *3*). On the lower surface of the film for the frequency $F_2 = 12$ T $n = 5, 6$ at $B = (2.7-2.15)$ T, and $n = 5.5, 6.5$ at $B = (2.4-2)$ T (Figure 4, curve *4*).

The obtained data on the position of the Landau levels n showed (Figure 4) that Landau levels are observed in higher magnetic fields in the film of n-$Bi_{1.92}In_{0.02}Te_{2.88}Se_{0.12}$, which is characterized by with higher cyclotron frequencies F_1 and F_2.

Berry phase value β (Figure 4, insert) in films of n-$Bi_{1.92}In_{0.02}Te_{2.88}Se_{0.12}$ (lines *1, 2*) and n-$Bi_{1.6}Sb_{0.4}Te_{2.91}Se_{0.09}$ (lines *3, 4*), is 0.58 and 0.47, respectively, and coincides for the upper and lower surfaces of the films and is located at the intersection of the lines *1, 2* and *3, 4* with the axis of the Landau indices n. The values of β are consistent with the experimental data of [17,25]. The change of the curvature of the cyclotron orbit, the Zeeman splitting [27] and the distortion of the linear dispersion of fermions with an increase of the magnetic field explain the discrepancies between the experimental values of the Berry phase β and the theoretical value which is equal to 0.5 in TI [19,25,28].

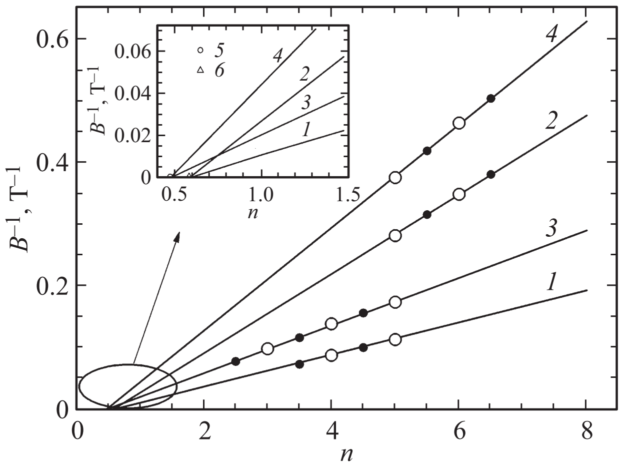

Figure 4. The Landau level indices n and Berry phase β in the reverse magnetic field B^{-1} obtained from the extremes of magneto-resistance oscillation amplitudes $\Delta\rho_{xx}(B^{-1})$, (Figure 2, *a* and *b*) in the film (curves *1, 2*) n-$Bi_{1.92}In_{0.02}Te_{2.88}Se_{0.12}$ and (*3, 4*) n-$Bi_{1.6}Sb_{0.4}Te_{2.91}Se_{0.09}$ for cyclotron resonance frequencies of F_1 (*1, 3*) and F_2 (*2, 4*). The Berry phase In the insert is β, calculated simultaneously with the Landau indices using LSM. *5* — $\beta = 0.58$ in films of n-$Bi_{1.92}In_{0.02}Te_{2.88}Se_{0.12}$ and *6* — $\beta = 0.47$ in n-$Bi_{1.6}Sb_{0.4}Te_{2.91}Se_{0.09}$.

5. Temperature dependences of resistance in a magnetic field

The temperature dependences of resistivity ρ in the temperature range of $(4.2-300)$ K in magnetic fields $B = 5$, 10 and 14 T were studied in films in n-$Bi_{1.6}Sb_{0.4}Te_{2.91}Se_{0.09}$.

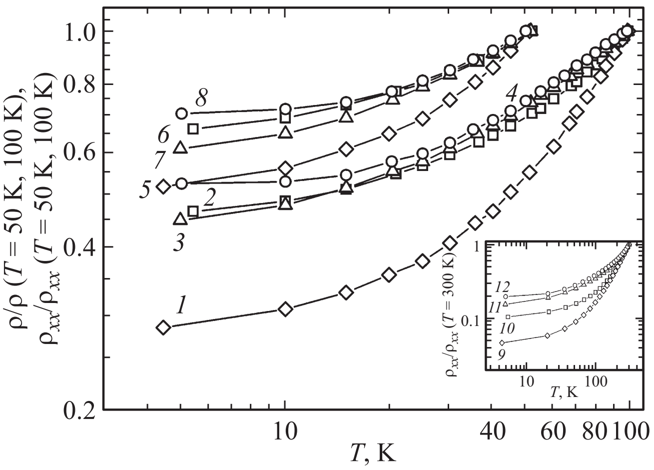

Figure 5. Normalized temperature dependences of resistance ratios to values ρ at temperatures 100 K (curve *1*), 50 K (*5*), 300 K (*9*) and resistance ρ_{xx}/ρ_{xx} $(T = 100\,\mathrm{K})$, (*2–4*) and ρ_{xx}/ρ_{xx}, $(T = 50\,\mathrm{K})$, (*6–8*) in magnetic fields B. The insert shows corresponding ratios at 300 K (*9–12*) for the film of n-$Bi_{1.6}Sb_{0.4}Te_{2.91}Se_{0.09}$. B,T: *1, 5, 9* — 0; *2, 6, 10* — 5; *3, 7, 11* — 10; *4, 8, 12* — 14.

Pronounced plateaus in the low temperatures at $T < 15\,\mathrm{K}$ (Figure 5, curves *4, 8*) were found on the normalized temperature dependences of the resistance ratios ρ_{xx}/ρ_{xx} $(T = 100\,\mathrm{K})$ and ρ_{xx}/ρ_{xx}, $(T = 50\,\mathrm{K})$ in the magnetic field $B = 14\,\mathrm{T}$. A plateau occurrence trend in the low temperature region at $B = 14\,\mathrm{T}$ was observed in case of the normalization of the ratios $\rho_{xx}/\rho_{xx}(T = 300\,\mathrm{K})$, but a formation of a complete plateau was not found (Figure 5, box).

The occurrence of such plateaus due to saturation of resistance with an increase in the magnetic field in [29] was explained by the impact of the surface states of Dirac fermions on transport properties as a result of the transformation of the bulk part of the material into an insulator in materials with strong spin-orbit interaction because of the preservation of symmetry with respect to time reversal.

Landau indices and Berry phase were determined in the region of magnetic fields, at which plateaus were observed on the normalized dependences of ρ_{xx}/ρ_{xx} $(T = 100\,\mathrm{K})$ and ρ_{xx}/ρ_{xx} $(T = 50\,\mathrm{K})$ on temperature, in the film of n-$Bi_{1.6}Sb_{0.4}Te_{2.91}Se_{0.09}$ (Figure 5, curves *4, 8*) (Figure 4, curve *3*). The minimum Landau index $n = 2.5$, which is characterized by a high population of fermions (Figure 4, curve *3*), and the non-zero Berry phase ($\beta = 0.47$) confirm the topological character of the identified plateaus in the studied TI films.

The ratio ρ_{xx}/ρ_{xx} (100 K, 50 K) increases on the plateau with an increase of the magnetic field to 14 T, however, the metallic type of conductivity in films n-$Bi_{1.6}Sb_{0.4}Te_{2.91}Se_{0.09}$ is preserved, unlike Bi_2Te_3 films, in which the type of conductivity changed from metallic to semiconductor with an increase of the magnetic field because of the topological metal-insulator phase transition [30].

A nonlinear dependence of resistance is observed in the studied films at low temperatures (Figure 5) ρ_{xx}/ρ_{xx} $(T = 100\,\mathrm{K})$ (curves *2, 3*) at $T < 15\,\mathrm{K}$ and ρ_{xx}/ρ_{xx} $(T = 50\,\mathrm{K})$ at $T < 20\,\mathrm{K}$ (curves *6, 7*) in magnetic fields at $B = 5$ and 10 T like in Bi_2Te_3 [28], that is, the ratios ρ_{xx}/ρ_{xx} $(T = 100\,\mathrm{K})$ and ρ_{xx}/ρ_{xx} $(T = 50\,\mathrm{K})$ decrease with an increase of the magnetic field from 5 to 10 T. Non-linearity was not found on dependencies ρ_{xx}/ρ_{xx} $(T = 300\,\mathrm{K})$ (curves *10–12*).

Nonlinearity at low temperatures in the ratios ρ_{xx}/ρ_{xx} $(T = 100\,\mathrm{K})$ and ρ_{xx}/ρ_{xx} $(T = 50\,\mathrm{K})$, accompanied by an increase of the magnetic field from 5 to 10 T, arises as a result of quantum interference effects, which are determined by the weak antilocalization of Dirac fermions in TI films with a long quantum phase coherence length l_ϕ [31–33]. The length of the quantum phase coherence l_ϕ increases with the decrease of temperatures, and $l_\phi \propto CT^{-m/2}$, where C is a constant for electron-electron and electron-phonon interactions $m = 3/2$ and 3, respectively. The value of l_ϕ is greater than the free path length l_F and reaches 300 nm in Bi films$_2$Te$_3$ [32] and 500 nm in Bi_2Se_3 [33] because of weak antilocalization of fermions in magnetic fields [31–33].

6. Conclusion

The parameters of the surface states of Dirac fermions in the layered films of n-$Bi_{1.98}In_{0.02}Te_{2.88}Se_{0.12}$ and n-$Bi_{1.6}Sb_{0.4}Te_{2.91}Se_{0.09}$ of TI were determined from the analysis of quantum oscillations of magnetoresistance measured in strong magnetic fields up to 14 T. It is shown that oscillations in films are characterized by two cyclotron resonance frequencies F_1 and F_2 because of different resonant conditions on the upper and lower surfaces. The surface concentration of Dirac fermions n_s, free-path length l_F and Fermi velocity v_F increase compared to n-$Bi_{1.6}Sb_{0.4}Te_{2.91}Se_{0.09}$ in film n-$Bi_{1.98}In_{0.02}Te_{2.88}Se_{0.12}$ with high power factor. An increase of the value of n_s indicates an increase of the impact of the surface states of fermions on the transport properties in films containing In.

From the analysis of the position of the minima and maxima of the amplitudes of quantum oscillations of magnetoresistance depending on the reverse magnetic field $\Delta\rho_{xx}(B^{-1})$, integer and half-integer indices of Landau levels n and the Berry phase are determined. It is shown that with an increase of the frequency of cyclotron resonance in the film of n-$Bi_{1.92}In_{0.02}Te_{2.88}Se_{0.12}$, Landau levels are observed in higher magnetic fields. The Berry phase β in films coincides for the upper and lower surfaces of films, and $\beta = 0.58$ and 0.47 for n-$Bi_{1.92}In_{0.02}Te_{2.88}Se_{0.12}$and n-$Bi_{1.6}Sb_{0.4}Te_{2.91}Se_{0.09}$ respectively.

The plateaus characteristic of TI were found in the film n-$Bi_{1.6}Sb_{0.4}Te_{2.91}Se_{0.09}$ on normalized temperature dependences of resistance $\rho_{xx}/\rho_{xx}(T = 50\,\mathrm{K})$ and

$\rho_{xx}/\rho_{xx}(T = 100\,\text{K})$ in magnetic fields $B = 14\,\text{T}$ at the low temperatures. The nonlinear dependence of resistance on the magnetic field at 5 and 10 T, associated with a decrease of resistance in the low temperature range, is explained by the weak antilocalization of Dirac fermions.

Conflict of interest

The authors declare that they have no conflict of interest.

References

[1] M.Z. Hasan, C.L. Kane. Rev. Mod. Phys. **82**, *4*, 3045 (2010).
[2] J.P. Heremans, R.J. Cava, N. Samarth. Nature Rev. Mater. **2**, *10*, 17049 (2017).
[3] P. Ngabonziza. Nanotechnol. **33**, *19*, 192001 (2022).
[4] M.J. Gilbert. Commun. Phys. **4**, *1*, 70 (2021).
[5] G. Jiang, J. Yi, L. Miao, P. Tang, H. Huang, C. Zhao, S. Wen. Sci. Rep. **8**, *1*, 2355 (2018).
[6] L. Zhang, J. Liu, J. Li, Z. Wang, Y. Wang, Y. Ge, W. Dong, N. Xu, T. He, H. Zhang, W. Zhang. Laser. Photon. Rev. **14**, *4*, 1900409 (2020).
[7] H. Liu, P.D. Ye. Appl. Phys. Lett. **99**, *5*, 052108 (2011).
[8] H. Steinberg, D.R. Gardner, Y.S. Lee, P. Jarillo-Herrero. Nano Lett. **10**, *12*, 5032 (2010).
[9] J. Zhu, T. Zhang, Y. Yang, R. Huang. Appl. Phys. Rev. **7**, *1*, 011312 (2020).
[10] Y. Chen. Surface excitonic thermoelectric devices. US Patent Application ID US20120138115A1 (2012).
[11] M. Eschbach, E. Młyńczak, J. Kellner, J. Kampmeier, M. Lanius, E. Neumann, C. Weyrich, M. Gehlmann, P. Gospodarič, S. Döring, G. Mussler, N. Demarina, M. Luysberg, G. Bihlmayer, T. Schäpers, L. Plucinski, S. Blügel, M. Morgenstern, C.M. Schneider, D. Grützmacher. Nature Commun. **6**, *1*, 8816 (2015).
[12] I.V. Korobeinikov, N.V. Morozova, L.N. Lukyanova, O.A. Usov, V.A. Kulbachinskii, V.V. Shchennikov, S.V. Ovsyannikov. J. Phys. D **51**, *2*, 025501 (2018).
[13] I.V. Korobeinikov, N.V. Morozova, L.N. Lukyanova, O.A. Usov, S.V. Ovsyannikov. Semiconductors **53**, *6*, 732 (2019).
[14] N.V. Morozova, I.V. Korobeinikov, S.V. Ovsyannikov. J. Appl. Phys. **125**, *22*, 220901 (2019).
[15] H. Liu, S. Liu, Y. Yi, H. He, J. Wang. 2D Mater. **2**, *4*, 045002 (2015).
[16] L. Bao, L. He, N. Meyer, X. Kou, P. Zhang, Z. Chen, A.V. Fedorov, J. Zou, T.M. Riedemann, T.A. Lograsso, K.L. Wang, G. Tuttle, F. Xiu. Sci. Rep. **2**, *1*, 726 (2012).
[17] S.Y. Matsushita, K. Ichimura, K.K. Huynh, K. Tanigaki. Phys. Rev. Mater. **5**, *1*, 014205 (2021).
[18] I.M. Lifshitz, A.M. Kosevich. Sov. Phys. — JETP **2**, *4*, 636 (1956).
[19] D. Shoenberg. Magnetic oscillations in metals. Ser. Monographs on physics. Cambridge University Press, Cambridge (2009).
[20] Y. Ando. J. Phys. Soc. Jpn. **82**, *10*, 102001 (2013).
[21] L.N. Lukyanova, O.A. Usov, M.P. Volkov. Semiconductors **53**, *5*, 620 (2019).
[22] L.N. Lukyanova, I.V. Makarenko, O.A. Usov. Semiconductors **56**, *5*, 317 (2022).
[23] L.N. Lukyanova, I.V. Makarenko, O.A. Usov. J. Phys.: Condens. Matter **32**, *46*, 465701 (2020).
[24] N.H. Tu, Y. Tanabe, Y. Satake, K.K. Huynh, P.H. Le, S.Y. Matsushita, K. Tanigaki. Nano Lett. **17**, *4*, 2354 (2017).
[25] S.-M. Huang, Y.-J. Yan, S.-H. Yu, M. Chou. Sci. Rep. **7**, *1*, 1896 (2017).
[26] S.K. Kushwaha, I. Pletikosić, T. Liang, A. Gyenis, S.H. Lapidus, Y. Tian, H. Zhao, K.S. Burch, J. Lin, W. Wang, H. Ji, A.V. Fedorov, A. Yazdani, N.P. Ong, T. Valla, R.J. Cava. Nature Commun. **7**, *1*, 11456 (2016).
[27] R. Dey, T. Pramanik, A. Roy, A. Rai, S. Guchhait, S. Sonde, H.C.P. Movva, L. Colombo, L.F. Register, S.K. Banerjee. Appl. Phys. Lett. **104**, *22*, 223111 (2014).
[28] A.R. Wright, R.H. McKenzie. Phys. Rev. B **87**, *8*, 085411 (2013).
[29] F.F. Tafti, Q.D. Gibson, S.K. Kushwaha, N. Haldolaarachchige, R.J. Cava. Nature Phys. **12**, *3*, 272 (2016).
[30] L.N. Lukyanova, Yu.A. Boikov, O.A. Usov, V.A. Danilov, M.P. Volkov. Semiconductors **51**, *7*, 843 (2017).
[31] H.-Z. Lu, S.-Q. Shen. Chinese Phys. B **25**, *11*, 117202 (2016).
[32] H.-T. He, G. Wang, T. Zhang, I.-K. Sou, G.K.L. Wong, J.-N. Wang, H.-Z. Lu, S.-Q. Shen, F.-C. Zhang. Phys. Rev. Lett. **106**, *16*, 166805 (2011).
[33] H. Peng, K. Lai, D. Kong, S. Meister, Y. Chen, X.-L. Qi, S.-C. Zhang, Z.-X. Shen, Y. Cui. Nature Mater. **9**, *3*, 225 (2010).

Translated by EgoTranslating